Interaction of multiple spiral rotors in a reaction-diffusion system

Hrishikesh Kalita and Sumana Dutta [*]

Department of Chemistry, Indian Institute of Technology Guwahati, Guwahati 781039, India

Rotors of reaction and diffusion are phase singularities that give rise to spiral waves of chemical activity, which are very similar to spatiotemporal patterns observed across several excitable media. Here we carry out experiments with the Belousov-Zhabotinsky reaction system and numerical simulations based on a reaction-diffusion model to show the possible interactions of multiple spiral rotors. When the cores of two spirals come very close to each other, they could either repel, attract, or remain stationary, depending on their relative chirality, phase, and distance separating them. Multiple pairs of spiral waves, in proximity to each other, could alter the paths of the individual rotors. A spiral core will be influenced most by the rotor that is closest to it, depending on the nature of the corresponding spiral wave arm. We observed rotors lying within a limiting distance of each other attract and annihilate. Otherwise, they push each other away until they reach a critical distance, beyond which all interactions seem to cease. We have established a relationship of this critical distance to the properties of the spiral wave. We also observed spontaneous symmetry-breaking instability for a system of up to eight rotors. Our experiments with the Belousov-Zhabotinsky reaction have successfully demonstrated the validity of the numerical results. A thorough understanding of the dynamics of several spiral rotors within a small area could help us perceive the nature of such excitation waves in cardiac tissue and cell membranes.

I. INTRODUCTION

Two-dimensional spiral waves and their three-dimensional counterparts, scroll waves, are responsible for arrythmia occurring in cardiac systems. The presence of such re-entrant waves are harbingers of tachycardia and fibrillation in the atria and ventricles of the heart, usually leading to fatal cardiac arrest [1–5]. These spiral rotors of electrophysiological activities share similar physics with spiral waves that occur in other excitable systems that span across physics, chemistry, biology, and geology [6–9].

The three-dimensional spatiotemporal dynamics of the heart is accompanied by a measurable scalar electrical value which can be recorded with an electrocardiogram (ECG). A rapidly drifting electrical rotor in the ventricles of the rabbit heart gives rise to complex excitation patterns manifested in an ECG as ventricular fibrillation (VF). A spiral rotor that gets pinned to an unexcitable heterogeneity will be akin to monomorphic ventricular tachycardia [10]. It has been shown that a single drifting rotor can cause fibrillation in smaller hearts. The human heart is, however, much larger, and VF occurs only in the presence of several such rotors. Hence, the interaction of multiple spiral rotors and the control of their dynamics is of interest to scientists across disciplines.

To date, numerous studies have been performed to achieve the repositioning and annihilation of spiral rotors [11–15]. The removal of spiral tips from an excitable media by non-invasive methods is a feat worth accomplishing. If one can remove rotating spiral and scroll waves from the cardiac sys-

tem, it will enable the medical community to better control the diseases related to these waveforms [16]. Existing studies have tried to control the dynamics of spiral waves by modifying the excitability of the system and applying external gradients and target waves [17]. Light [11,12] and electric field [13] have been used to move the tips of the spirals in a two-dimensional reaction-diffusion system, sometimes leading to annihilation of the waves. High-frequency wave trains have been successfully used to force spirals into defect drifts [18]. Using multiple wave fields, several rotors could even be localized to a particular position. The interaction of rotors in both two and three dimensions with system inhomogeneities have also been a subject of intense study. Theoretical as well as experimental investigations have revealed how the frequency, position, phase, and nature of spirals can get modified in the presence of inhomogeneities [19–22].

There are some examples of spiral interaction in existing literature. Experimentally, instances of suppression and expulsion of one spiral tip by another were observed in the aggregation of *Dictyostelium* amoebae [23]. Some studies of the interaction of phase singularities (spirals) in the cardiac model are also available [24]. This study demonstrated that a spiral competition instability was responsible for the symmetry breaking of the spiral pair. Numerical studies on the FitzHugh-Nagumo model showed that both like as well as unlike charged spiral vortices (topological charges) can form bound pairs possessing either an axis or a center of symmetry [25]. This charge is attributed to the chirality or the sense of rotation of spiral waves. Corotating spirals are considered to have like charges, and counterrotating spirals are said to be oppositely charged. In yet another study with the complex Ginzburg-Landau equations, it was established that

———————
[*]sumana@iitg.ac.in

the interaction between well-separated spirals in the particular system is exponentially weak and does not depend on the topological charges [26]. Symmetry-breaking instabilities in a bound state of a spiral pair can also induce the expulsion of one spiral [27], sometimes leading to its elimination at the system boundary [28]. A numerical study of the light-sensitive BZ medium demonstrated how light intensity can modulate the behavior two counterrotating spirals [29]. In a recent numerical study of the Ferroin-catalyzed BZ system, it was shown that a spiral wave interacting with its axis-symmetric mirror image undergoes attraction when within close distances leading to annihilation, followed by repulsion and finally a region of extremely slow drift, as the distance separating them increases [30]. However, such studies on the interaction of spiral rotors are mainly limited to a pair of spirals. Numerical studies on model systems were also expanded to multiarmed vortices [31]. Weijer *et al.* demonstrated from extensive simulations that spirals having same chirality, with tips less than one wavelength apart, can form multiarmed spirals [32].

In three dimensions, experiments with coplanar scroll rings demonstrated that their filaments undergo crossover collision and reconnect when they are within a core length of each other [33,34]. On the other hand, the filaments repelled when placed over one another. In yet another study of straight, parallel scroll waves, it was established that the filaments repelled only when the interfilament distance was shorter than the wavelength of the scroll waves [35]. When this distance was almost equal to the wavelength, the two scroll waves synchronized.

A detailed study on the interaction of multiple (more than two) spiral vortices with identical frequencies, showing spontaneous annihilation and repulsion, and also establishing the exact distances at which the nature of the interaction changes, is yet to be carried out. It remains to be seen if the limiting distances for the interaction of several spiral rotors are exactly the same as that for a pair of spiral tips, or they differ [30]. If they do differ, we aim to understand the causes of such variation.

In the current paper we revisit the problem of spiral wave interaction and extend it further. By employing numerical as well as experimental methods, we explore the dynamics of multiple spiral rotors around each other. We show with experimental evidence spontaneous annihilation of vortices (without employing any external force). We carry out detailed simulations with the Barkley model, for one, two, and four spiral pairs, by varying the mutual distances between them. It is observed that, with increasing distance between the rotors, attractive potentials become repulsive. Our simulations reveal different interaction zones with a transition from an attractive to a repulsive zone and a further transition from this repulsive zone to a zone of no interaction. The important role of the wave connecting two rotors has also been established. We additionally carried out experiments in thin layers of a chemical reaction-diffusion system. We have chosen the Ferroin-catalyzed Belousov-Zhabotinsky (BZ) [7] reaction for the study of the spiral dynamics. Several experiments have been carried out, varying the distances between pairs of spiral tips. Our experimental results corroborate well with the numerical predictions. The phenomena of spiral repulsion and

spiral attraction leading to annihilation have been successfully demonstrated, for a system of up to eight rotors. Additionally, several intriguing observations have been made for a system of multiple spiral tips, like spontaneous symmetry breaking.

II. NUMERICAL MODEL

The generic two-variable Barkley model is often employed for the study of reaction-diffusion systems [36]. We have chosen this model for our study as it is quite versatile and can be applied to different experimental systems. It has been widely used to explore the dynamics of spiral and scroll waves in the BZ system [13,37,38]. The Barkley model is also closer to the FitzHugh-Nagumo model, often used to model the cardiac waves.

In the presence of diffusion, the Barkley model can be written as

$$\frac{\partial u}{\partial t} = \frac{1}{\epsilon}\left[u(1-u)\left(u - \frac{v+b}{a}\right)\right] + D_u\nabla^2 u, \qquad (1)$$

$$\frac{\partial v}{\partial t} = (u - v) + D_v\nabla^2 v. \qquad (2)$$

Here u is the activator and v the inhibitor. In the BZ system, u and v are qualitatively related to the concentrations of bromous acid and the oxidized form of ferroin, the catalyst, respectively. $D_u = D_v = 1.0$ are the diffusion coefficients of the two species. For our simulations, we have chosen the parameter values of $a = 0.84$, $b = 0.07$, and $\epsilon = 0.02$. In chemical reactions, most species diffuse with approximately the same diffusion coefficient [36], supporting our choice of equal diffusion coefficients. This, along with our parameter set, describes a system in which spiral and scroll waves undergo rigid rotation [20,39], as is the case with our experimental system for the chosen chemical recipe. A time interval of $\Delta t = 0.012$ time units and a step size of $\Delta x = 0.35$ space units were chosen. We employed no-flux (Neumann) boundary conditions on all sides.

The two-dimensional space (of area 105×105 space units) was divided into 300×300 cells, of dimension 0.35×0.35 (space units) each. A five-point Laplacian stencil was used to discretize the space. For initiating a pair of spiral waves, the concentrations of u and v are taken to be 0.0 across the entire space, except for a thin strip in the middle. Here three long strips of isoconcentration lines (with a width of two cells or 0.7 space units each), representing the front ($u = 0.9$, $v = 0$), middle ($u = v = 0.7$), and back or refractory area ($u = 0$, $v = 0.9$) of the wave, are taken as the initial conditions for starting a plane wave. The length of the strip was varied from experiment to experiment and ranged from 10 cells or 3.5 space units to 110 cells or 38.5 space units. Our rotors are initiated far from the system boundary.

Using an explicit finite difference method for space we converted the system of partial differential equations into ordinary differential equations and proceeded to integrate them by employing the fourth-order Runge-Kutta method. Simulations were repeated using a nine-point stencil, yielding the same results. This choice of parameter values and identical diffusion coefficients can initiate and sustain stable, nonmeandering spirals, with a circular core of diameter $d_s = 1.8$ space units. The average wavelength of the spirals (λ) far
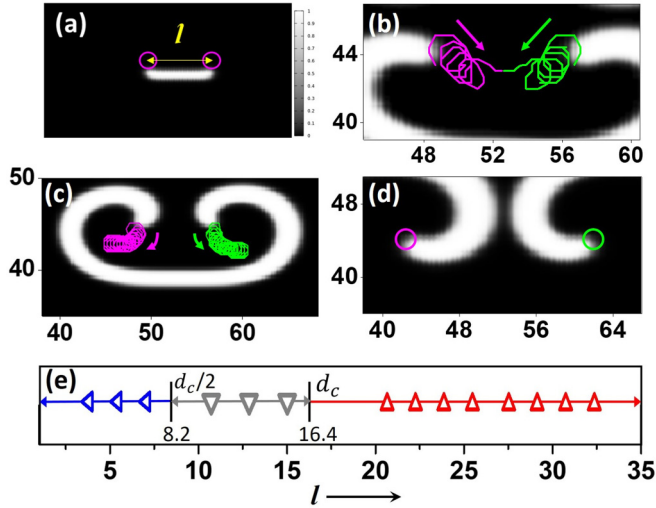
FIG. 1. Interaction between the two cores of a spiral pair. (a) Snapshot of an initial waveform at 0.48 time units after initiation. It is a grayscale image of the activator u, as shown in the color bar. Hence, the white regions represent areas of heightened wave activity. (b) Attraction leading to annihilation for $l = 6.65$ space units, and (c) repulsion between the spiral rotors, for $l = 9.25$. (d) No motion of the rotors for over 1000 rotations for $l = 19.75$. (e) Phase diagram of interaction between the two cores in a spiral pair. The open triangles depict the type of interaction for a given simulation with fixed l value. Blue left-pointing triangles portray attraction and annihilation [like in (b)], gray downward-pointing triangles depict repulsion [like in (c)], and the open red upward-pointing triangles represent the absence of any interaction between the two rotors [as in (d)]. d_c depicts the critical distance of interaction.

from the core is around 18.2 space units, while the average time period is 5.3 time units. The wavelength (as well as the time period) is measured from the time-space plot, by averaging over several wavelengths (periods) [17]. The spiral tip is defined as the intersection of the isoconcentration lines, $u = 0.5$ and $v = a/2 - b = 0.35$ [18,36].

III. NUMERICAL RESULTS AND DISCUSSIONS

We begin our simulations with the simplest case: a single spiral pair. These are two counterrotating spirals, with the same initial phases, and they arise out of a single plane wave. Please refer to Fig. 1(a) for visualizing the initial wave form and Fig. 1(c) for one such pair of counterrotating spirals, generated from this initial plane wave. We refer to these two spiral rotors as initially joined by a wave.

The distance between the centers of the two circular cores of the spirals, measured after the first rotation, is considered to be the initial length l. When (l) is quite large, e.g., $l = 19.75$ space units in Fig. 1(d), the two spirals keep on rotating around their circular cores. There is no visible or measurable movement of the spiral cores, even after thousands of rotations. As the cores are brought closer, we can observe an immediate repulsion between them, which pushes them apart, till the distance between them is a little less than one wavelength. Here they continue rotating around a fixed circular orbit. Figure 1(c) shows one such experiment, where the initial

value of l is 9.25. However, in this case the right tip travels a little lower than the left one, breaking the symmetry slightly. As we keep decreasing the initial distance between the cores, this repulsion phenomenon is observed until $l = 8.2$, below which there is a sudden change from repulsive behavior to an attractive one. In Fig. 1(b), an example of attractive interaction between the cores of a spiral pair, which are initially 6.65 space units apart, is seen. The two vortices are observed to trace a curved path that brings them close together and finally annihilate. It is to be noted that 1.8 space units is the diameter of a noninteracting spiral core for the chosen parameter range. Hence, we observe for this numerical experiment [Fig. 1(b)] that though the value of l is many times the core diameter $l > 3.6 \times d_s$, still the spiral rotors do attract each other and eventually annihilate. The annihilation of two counterrotating spirals that lie within one core length of each other had been previously observed in the literature [25]. However, in our study, we find that the spirals attract even when they are farther away, as long as they are less than 8.2 space units apart. When the distance between the spiral tips is less than 4.9 space units, the spiral rotors do not complete one full rotation. Instead, their strong mutual attraction forces them to annihilate before that. In all our simulations, we measure the value of l by considering the position of the centers of the individual rotors, if an invisible boundary existed between the two tips, stopping their interaction.

A phase diagram constructed on the behavior of two interacting spiral cores is shown in Fig. 1(e). There are three clearly marked regions in the phase diagram, one of attraction leading to annihilation ($8.2 > l$), repulsion ($16.4 \geqslant l \geqslant 8.2$), and no interaction ($l > 16.4$). Interestingly, we may observe that when $l > \lambda - d_s = 16.4$, the spirals do not interact. Let us call this value the critical distance, d_c. On the other hand, the interaction changes from repulsive to attractive at exactly half of this critical value, i.e., $l = \frac{1}{2}(\lambda - d_s) = 8.2$. Two counterrotating spirals initiated from the same wave begin to rotate at a maximum distance ($l_{max} = l + d_s = 20$), and then come closer to each other as the two tips rotate in. This means that the maximum distance l_{max} between the two spiral tips must be more than one wavelength ($\lambda = 18.2$ space units) for there to be no interaction between them. In our numerical system, whenever there was any motion of the spiral core, that happened from the beginning (right after initiation) till that time when the spiral rotors attracted each other and eventually got annihilated, or reached a distance where the movement ceased. This is similar to the observations made in [30] where the authors report that a spiral attracts its mirror image on a no-flux boundary when the distance between them is less than 0.28λ, they repel beyond that till a distance of 0.82λ, and then there is a very slow drift. Additional spiral-tip dynamics, of the examples shown in Fig. 1, elucidating the change of the tip position with time can be observed in the Supplemental Material Fig. S1 [40].

Next, we carry out simulations with two spiral pairs (a four-rotor system). We initiate this system of four rotors, by placing two plane parallel waves, with their refractory zones or wave tails facing each other [Fig. 2(a)]. As the wave expands, two pairs of counterrotating spirals are formed. The two spirals which are created at either ends of a plane wave are referred to as spiral twins, and the initial distance between the centers
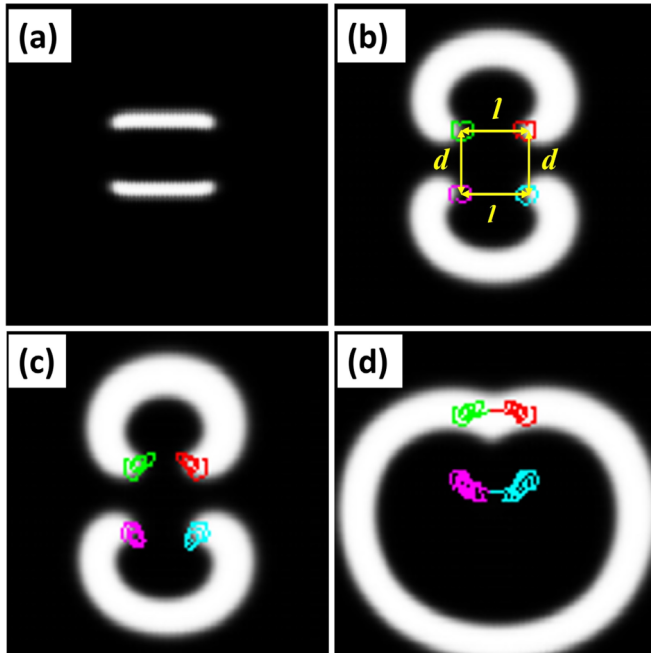
FIG. 2. Interaction of two spiral pairs showing attraction and annihilation. Snapshots of spirals along with tip trajectories at $t =$ (a) 0.48, (b) 7.2, (c) 18.0, (d) 31.2, in normalized time units. The colored curves are the tip trajectories. Each tip has been assigned a unique color for better visualization. The initial horizontal intertip distance $l = 7.4$ (yellow horizontal straight lines) and initial vertical distance between cores $d = 7.0$ (yellow vertical straight lines) are marked in (b). Area of each snapshot is 35 space units × 35 space units.
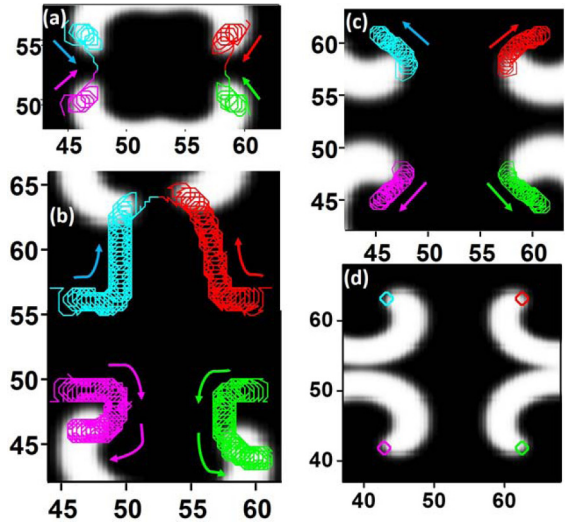

FIG. 3. Interaction between pairs of spirals. Tip trajectories superimposed on the snapshots (chosen from the later half of the trajectory) showing (a) vertical annihilation for both pairs, where initially, $l = 15.75$ and $d = 6.3$. (b) Simultaneous repulsion between one pair and annihilation between the other, for $l = 14.35$ and $d = 7.0$. (c) Repulsion between all rotors when $l = 10.15$ and $d = 9.8$. (d) No interaction for $l = 19.3$ and $d = 21.2$. Movies of the simulations are available in the Supplemental Material [40] (Mov3a–Mov3d).

of their cores is defined as "l" [Fig. 2(b)]. The initial distance separating a spiral core from its nearest neighbor (other than the twin) is defined as "d." For the case of two spiral pairs or four rotors, we place the two plane waves along the horizontal (hence l is the horizontal distance between two neighboring rotors and d the vertical distance). We can also place l along the vertical direction and still obtain exactly same results, as is demonstrated by plots of trajectories of some additional simulations (see Fig. S2 [40]).

For studying a system of four spiral rotors, we initiate a completely symmetrical arrangement so that the lines joining the centers of every rotor to its nearest neighbors will form a rectangle (square for equal l and d values). We carried out several simulations by varying the initial horizontal distance between the cores (l) and the vertical nearest-neighbor distance (d). By doing so, we observed different kinds of synergistic phenomena between the spiral tips.

Figure 2 depicts an example, where mutual collapse occurs between the cores of a spiral pair, due to annihilation along l. We later refer to this kind of annihilation as horizontal annihilation, for a system of two spiral pairs. The trajectories superimposed on the snapshots are the paths traced out by the tip of the spiral waves. It helps us get an idea of the movement of the spiral rotor. As time progresses, the tips get closer, indicating an attractive interaction between the two cores of the initially formed spiral pairs.

An individual spiral tip is influenced by all rotors close to it. For a system with two spiral pairs initially facing each

other, there are two rotors nearest to an individual spiral tip: one placed along l, that is, at the far end of the initial mother wave, and the other rotor is placed along d, that belongs to a neighboring spiral wave pair. In this example, $l = 7.4$ space units and $d = 7.0$ space units, both smaller than the limiting distance, $\frac{d_c}{2} = 8.2$. Here, even though l is larger than d, the spirals choose to attract horizontally, along the distance l. This unexpected dynamics of the spiral tips requires more exploration.

Figure 3 shows all other kinds of possible interactions between spiral pairs, as the l and d values are varied. Figure 3(a) is another instance of annihilation of vortices, between two spiral pairs facing each other. Two spiral tips that initially belong to different spiral pairs start attracting each other, along the vertical distance d, until they finally annihilate each other. This event is later referred to as vertical annihilation. The spiral rotors may have chosen a vertical annihilation over the horizontal in this example, because of the very low value of d (=6.3) as compared to l (=15.75), the latter 2.5 times the value of d.

Figure 3(b) illustrates some remarkable phenomena. Here $l = 14.35$ and $d = 7.0$. Even though l is still quite larger than d ($l = 2.05 \times d$), we can observe an initial attraction along l, for both spiral pairs. After covering a certain distance, however, the spiral rotors become strongly repulsive, and start moving in the vertical direction, away from the middle. For the bottom pair, this results in a complete U turn, as the two spiral tips initially approach each other, turn in the negative y direction, and after a while again start moving horizontally apart. On the other hand, in the top pair, after initially attracting horizontally for a while, they start moving away in parallel (like a bound state) towards the positive y direction,
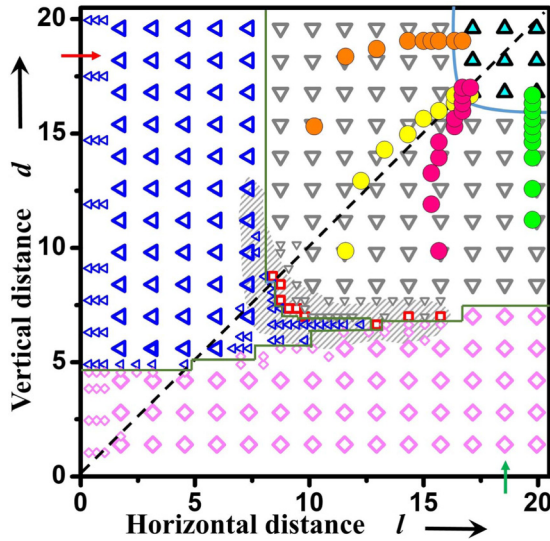
FIG. 4. Phase diagram of interaction between two pairs of spirals. The triangles, diamonds, and squares depict the type of interaction for a given simulation with fixed l and d value. Open magenta diamonds depict vertical annihilation, the open blue left-pointing triangles depict horizontal annihilation, gray downward-pointing triangles depict repulsion, and the cyan-filled black-bordered upward-pointing triangles depict no interaction between any rotor. The red squares are the cases where one of the pairs attracts and annihilates, while the other pair repels and moves away from each other. The various regions have been separated by solid lines, which are only qualitative in nature. The shaded region denotes the occurrence of the complicated dynamics of spiral tips as in Figs. 3(b) and S3 [40]. Four numerical experiments have been traced here, with the changing l and d value of their spiral cores depicted by closed colored circles of a unique color. It shows how the rotors move from different zones of repulsive interaction, into the noninteracting zone. The red and olive arrow mark the $d = 18.2$ and $l = 18.55$ lines, respectively.

before attracting each other once again, finally leading to the annihilation of the spiral pair. This is a very good example of a symmetry-breaking instability. It indicates a cooperative effect among the spirals. It is noteworthy that the value of d here is smaller than $\frac{1}{2}d_c$, which would point towards an attractive interaction in the vertical direction, in a simpler situation (a single spiral pair). Nonetheless, for a system of four rotors, the tip of a spiral wave is influenced by multiple rotors. This modifies its trajectory, and we often end up with such complicated dynamics and spontaneous symmetry breaking.

In Fig. 3(c), $l = 10.15$ and $d = 9.8$, both values greater than $\frac{d_c}{2}$. Here initially the repulsion is vertical, but after some time the tips start tracing almost diagonal trajectories away from their initial positions. With very high d and l values, the dynamics of the waves become independent of each other (no interaction), as seen in Fig. 3(d), where $l = 19.3$ and $d = 21.2$, both greater than the critical distance d_c.

Figure 4 summarizes the results of all our numerical experiments with two spiral pairs. As was observed in the results of Figs. 2 and 3, spiral tips are influenced by all rotors lying in their vicinity, leading to a plethora of tip dynamics. Since we start with two identical spiral wave pairs, facing each other, so

we try to compare between the attraction or repulsion faced by a rotor due to its spiral twin and the other rotor closest to it, which belongs to a different pair of spirals. This phase diagram gives us a better understanding of the interactive effects between the spiral rotors. When the distance between two rotors is very low, they show strong attraction towards each other leading to mutual annihilation. Depending on the values of l and d, they attract either horizontally or vertically. It is observed that for all d values less than 4.9 space units, the spirals undergo vertical annihilation. As mentioned earlier, this is the minimum distance of separation of a spiral rotor from its neighbors, to complete one full rotation. As the plane waves start curling in, one spiral rotor encounters its neighbor from the other spiral pair, before it comes into the vicinity of its own twin. So, when the d distances are low (<4.9), they annihilate vertically even before they can complete the first rotation (see Fig. S4 for a representative example of tip trajectory in this case [40]).

With increasing l and d values, there is a transition from attractive zone to the repulsive zone. However, the phase diagram is asymmetric, along a diagonal line (broken line in Fig. 4) drawn across $l = d$. This can be attributed to the difference in the strength of interaction, specifically attraction (as the noninteractive zone is symmetric along the diagonal), between the two kinds of neighbors. As the system transitions, the highest value of d for which vertical annihilation is found is seven space units, whereas horizontal annihilation was observed for l values as large as 12.25. The higher limiting values of l as compared to d for attraction leading to annihilation (horizontal and vertical, respectively) indicate some kind of stronger attractive power between spirals that are initially joined by the same wave and warrant further investigation.

We have already mentioned that change of coordinates does not change the relationship between the spiral tips. Additional simulations by initiating two pairs of spirals in the vertical direction, where l lies parallel to the y axis, shows that the phase diagram remains unchanged for any orientation of the spirals, as long as their relative l and d distances are maintained. Comparative results for these two kinds of simulation can be found in the Supplemental Material (Fig. S2 [40]). This confirms that our observations do not arise from any numerical error or bias along a particular direction. Rather, in both these kinds of simulations (as well as all our experiments reported later), we have initiated a pair of waves, which have their trailing edges facing each other (see Fig. S5 for a detailed explanation of the wave motion [40]). This results in an inhibition of attractive interaction between the initial waveforms. If the initial waves are horizontally placed, there would be an inhibition along d. Eventually, when the waves expand and merge, the new vertical waves move towards each other, with their leading edges facing one another. This results in a comparatively stronger attraction of the spiral rotors along l. This is the reason for our observation that one spiral is more attracted towards its twin (born from same initial wave). Changing the direction of wave head and its repolarizing tail would reverse our observations. If the leading edges of the initial horizontal waves would face each other, they would attract more along the vertical, resulting in a stronger attractive interaction along d. Some examples are given in Fig. S2(c) [40]. For such a system, the spirals will not be more strongly

attracted by their twin, but by their other nearest neighbor, hence resulting in a higher limiting value (for attraction followed by annihilation) for the vertical d distance than the horizontal l distance. We would also expect the phase diagram (Fig. 4) to change for such a system.

In Fig. 4 the transition from attraction to repulsion cannot be defined by a sharp (l, d) line; instead it is a thin region (shaded area in Fig. 4) within a range of l and d values. The systems in the transition region could have three kinds of interactions: the spirals may attract and annihilate, they might all repel, or there could be a case of simultaneous attraction and repulsion in the system (depicted by the red squares in Fig. 4). Figure 3(b) is an example of such mixed dynamics. This unusual dynamics arises due to the symmetry-breaking cooperative effect of the spiral waves. The relative motion induced by this effect is quite complicated and may often give rise to completely unexpected dynamics. Tip trajectories for one such experiment ($l = 12.95$, $d = 6.65$) can be found in the Supplemental Material [40] (Fig. S3). There are also some points where l is greater than half the critical distance, like for $l = 10.2$ and $d = 6.3$, where horizontal annihilation is observed (Fig. S5 [40]). Although for this particular point $l = 1.6 \times d$ and $l > \frac{d_c}{2}$, whereas $d < \frac{d_c}{2}$, still the spirals approach along l and annihilate. Again this shows that the spiral vortices feel a stronger attraction for their horizontal neighbor (when initiated in this way), rather than other neighbors which may be closer to them. However, the presence of the other spiral pair enables this horizontal annihilation between the tips of the spiral wave, which would not have been achieved for a single spiral pair having $l > \frac{d_c}{2}$. Barring these few exceptions, for $l > \frac{d_c}{2}$ and $d > \frac{d_c}{2}$, there exists a large zone of spiral repulsion. With further increase in the vertical and horizontal distances (beyond d_c), all interaction vanishes. Here, from the repulsive to no-interaction zone, the transition is very sharp with clear (l, d) demarcating lines, along the critical distance (16.8 space units).

We have additionally traced the trajectories of four numerical experiments in Fig. 4 (marked by full circles). All the points lie in the repulsive zone at their initiation and are traced till that point, where the relative motion of the tips ceases. One may observe that the l and d values change spontaneously toward the zone of no interaction. When both distances are much smaller than the critical value of 16.4 space units, for, e.g., the yellow circles which start from (11.55, 9.8), the vertical as well as the horizontal distance increases, as the pairs move toward the zone of no interaction (16.4, 16.4). They, however, do not trace an exact straight line. The vertical distance (d) increases faster than the horizontal (l), as seen from the curved path of the yellow circles. This points towards the stronger repulsion of the trailing edges of the horizontal waveforms, along the vertical, when the rotors are linked to the spiral arm of their initial twin, thus separating them vertically. On the other hand, when one of the initial distances is beyond the critical distance, e.g., the experiment depicted by the green circles, where the initial distances are (19.4, 11.2), only the other distance (vertical in this case) increases all along the path until it reaches the noninteracting zone.

Comparison of the phase diagrams of single and double spiral pairs [Figs. 1(e) and 4] show some similarities and some dissimilarities. A careful observation of Fig. 4 reveals that, for a fairly large value of d (>16.4), the system is in the no-interaction zone in the vertical direction. Again, for $l > 16.4$, it reaches the no-interaction zone in the horizontal direction. For both these conditions, the individual pair of spirals that lie close by behave as they would in the absence of any other rotors (as in Fig. 1). In the case of the former ($d > d_c$), as l increases (for, e.g., along $d = 18.2$ marked by a red arrow in Fig. 4), we can observe horizontal annihilation followed by repulsion and then no interaction. Similarly, in the latter case ($l > d_c$), vertical annihilation is followed by repulsion and no interaction, as d value is raised from small to large (for, e.g., along $l = 18.55$ marked by an olive arrow in Fig. 4). The presence of the neighboring rotors for lower d and l values brings about the complicated dynamics observed in the system [Figs. 3(b), 3(c), S3, and S5]. From this observation, we may wonder if an increase in the number of interacting spiral cores might lead to more intricate dynamics.

Towards this aim, we extended our system to eight spiral cores. We designed a very symmetrical system of spirals, in order to be able to clearly observe any symmetry-breaking dynamics. Figure 5(a) depicts such a system. In Fig. 5(b) we again define our distance parameters l and d as the initial distance between the cores in a spiral pair, and shortest distance between two nearest cores belonging to different spiral pairs, respectively. We initiate four spiral pairs having the exact same dimensions, and spaced equally apart, forming a kind of closed system, with a fourfold degeneracy in the initial wave forms [Fig. 5(a)].

In such a symmetric system, we observe mainly four kinds of interactions. A sample of each type is illustrated in Fig. 5. Figure 5(c) shows mutual annihilation between diagonal pairs of spirals, due to a small d ($= 6.9$) value, as compared to l ($= 10.1$). Here each of the spiral pairs behaves almost symmetrically. In Fig. 5(d), $l = 9.0$ and $d = 7.7$. Here both annihilation as well as repulsion is observed simultaneously. The loss of symmetry in this case is probably occurring due to a symmetry-breaking cooperative effect. The spiral pairs travel like bound states for a distance, before the asymmetry sets in, making some pairs repel, and others attract and annihilate. This case is similar to that seen in the case of two spiral pairs [Fig. 3(b)]. Figure 5(e) shows the repulsion of all the spirals. Here $l = 9.5$ and $d = 12.5$, both larger than $\frac{1}{2}d_c$. Although their direction of transition is quite symmetric, the velocity is different for different rotors. Some spirals have traveled larger distances compared to others, in an equal amount of time. Hence, the repulsion experienced by all the spirals are not uniform throughout. When the spirals are farther away from each other, they do not show any visible interaction, as depicted in Fig. 5(f), where $l = 16.8$ and $d = 23.2$.

Preliminary studies with corotating spirals show similar trends in their interaction. Spirals with the same sense of rotation cannot annihilate each other [25,35], as they carry similar topological charges. When within close proximity, they interact depending upon their initial phases. Corotating spiral tips, initiated with the exact same phase, repel each other, till they are separated by a critical distance, close to the λ value. This is observed even when they lie within one core diameter of each other. However, when they are initiated
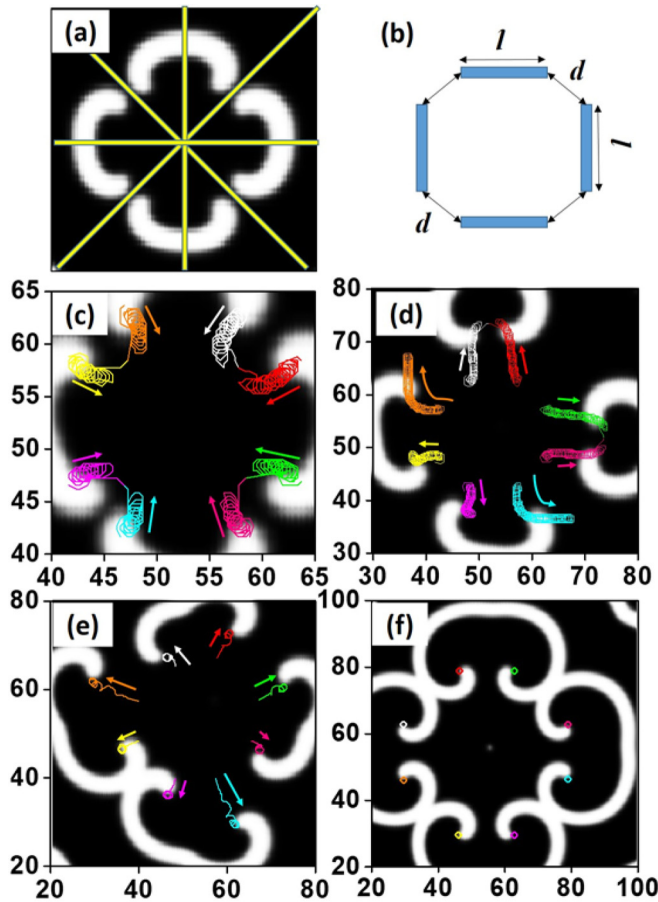
FIG. 5. Interactions between four pairs of spirals. (a) Snapshot of one numerical experiment at $t = 40.8$ normalized time units, for $l = 10.1$ and $d = 6.9$ normalized space units. (b) System design showing the initial placement of waves and corresponding definition of d and l in these cases. (c) Tip trajectory for $l = 10.1$ and $d = 6.9$. (d) Tip trajectory for $l = 9.0$ and $d = 7.7$. (e) Tip trajectory for $l = 9.5$ and $d = 12.5$ (for the purpose of simplicity, only tip positions at intervals equal to the time period of the spirals, 5.34 time units, are shown here). (f) Tip trajectory for $l = 16.8$ and $d = 23.2$. Movies of the simulations are available in the Supplemental Material [40] (Mov5c–Mov5f).

with a significant phase difference, such corotating spirals can form coupled pairs, often with complicated trajectories [32].

IV. EXPERIMENTAL METHODS

The BZ reaction system provides a convenient way to study the behavior of spiral waves experimentally. A suitable concentration range that sustains spirals was chosen for our experiments. The final concentrations of the reactants are $[H_2SO_4] = 0.2$ M, $[NaBrO_3] = 0.04$ M, [malonic acid] = 0.04 M, and [ferroin]= 0.001 M. We prepare a homogenous mixture of 0.8% (w/v, final concentration) agarose gel in millipore water (having resistivity of 18.2 MΩ cm), with constant stirring and moderate heating. Then it is allowed to cool slightly with continued stirring so as to keep the mixture homogeneous throughout. Now the other reactants (in water) are added to the stirred solution sequentially. When the

mixture is just above the gelling temperature, it is poured into a Petri dish of 8 cm diameter and is allowed to cool. The BZ gel layer has a thickness of 2 mm. All experiments are carried out at room temperature (22 ± 1 °C). The reaction system was illuminated from below by using a diffused, cold white light source (Dolan Jenner DC950H). We observe the reaction mixture from above with a charge coupled device camera (mvBlueFOX 22a), which is connected to a personal computer. A blue dichroic filter was attached to the camera for better imaging. We recorded the images at 2 s intervals. The spiral tips were detected by analyzing the snapshots using an in-house interactive program written in the MATLAB platform. The tips were recognized as the points near the spiral head with the highest curvature. In the presence of aerial oxygen, the excitability of the BZ system reduces with time, the waves become slower, and the time period increases [41]. However, we have covered our reaction to minimize this effect. Moreover, we use only experimental data recorded during the first 3 h after initiating the reaction. During this period, the wavelength and time period of the waves do not change.

The recipe of the BZ reaction that was chosen for these experiments generated a rigidly rotating spiral wave with core diameter $d_s = 0.09$ cm, an average wavelength, $\lambda = 0.48$ cm, and a rotation period of 367 s. The wavelength and time periods were measured just like in the case of the numerical simulations, as depicted in [17]. A single spiral pair was generated in the usual way by cleaving a circular wave with a thin glass plate. In order to generate two pairs of spirals, first two circular waves are initiated in close proximity of each other, by dipping two silver wires (Aldrich 99.9% purity) into the reaction gel for a few seconds. The silver helps in catalyzing the reaction, and hence initiates a circular target wave. The waves are allowed to expand and to come closer together. Finally, they are cleaved in such a way that we generate two pairs of spirals, facing one another. The system of spiral waves generated in this manner is similar to what we obtain for our numerical simulations [Fig. 2(b)]. Though the initial waveforms in our experiments were curved [Fig. 6(b)], instead of straight [Fig. 2(a)], the direction of their rotation is the same as that of our numerical simulations. The leading edge of the two initial waves move away from each other. The distance between the circular waves at the time of cleaving has a special importance as the value of d, or the vertical distance between the center of the spiral cores, depends on it. One more important parameter is the horizontal distance between the centers of the two spiral cores in a pair generated from a single circular wave, l. Special care was taken to maintain these distances, by ensuring that the initial target waves are of the same size, and they are cut almost at the same time, so as to obtain similar d and l values between both pairs.

V. EXPERIMENTAL RESULTS

Our simulation results for two spirals (Fig. 1) were verified by our experiments with a single excitation wave having two counterrotating spirals at either end. We have designed a phase diagram for a pair of spirals in an experimental system [Fig. 6(a)], in keeping with the results of the numerical simulations, in order to graphically demonstrate the various kinds of interactions observed in our experiments. The critical
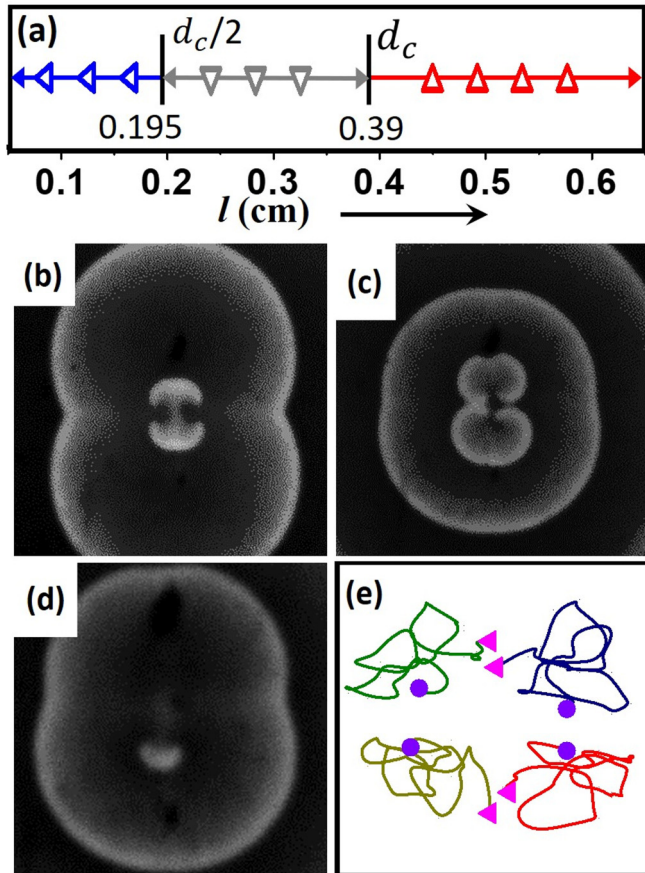
FIG. 6. (a) Phase diagram of interaction between the two cores of a spiral pair in experiments. Blue left-pointing triangles depict annihilation, gray downward-pointing triangles portray repulsion, and the open red upward-pointing triangles represent the no interaction between the two rotors. (b)–(e) Annihilation of two pairs of spiral waves. Snapshots at (b) 8.47 min, (c) 27.28 min, and (d) 32.14 min after initiation of the reaction. Area of each snapshot is 2.95 cm × 2.95 cm. (e) Tip trajectories (colored curves) showing attraction and annihilation. The trajectory of each tip has been given a unique color for the purpose of clarity. Closed purple circles designate the initial position of every individual rotor, and the cyan triangles are the final positions prior to the moment of annihilation (at 27.33 min). Area shown in box is 0.55 cm × 0.55 cm. Initially, $d = 0.14$ cm, $l = 0.185$ cm. A movie of this experiment is available in the Supplemental Material [40] (Mov6).

distance, $d_c = 0.39$ cm, is one beyond which all interactions cease, and the distance $d_c/2$ marks the switch between repulsion and attraction. Analyzing with respect to the wavelength and core size, as we did in our simulations, here the critical distance of interaction is equal to $d_c = \lambda - d_s = 0.48 - 0.09 = 0.39$ cm. So, the intercore distance below which we should observe annihilation is expected to be $\frac{1}{2}d_c = 0.195$ cm. Here we discuss the systems with a higher number of rotors. We carried out a series of experiments with two pairs of spirals, by varying the distances d and l, that allowed us to observe the different kinds of interactive phenomena predicted by the simulations. We discuss representative examples of each kind here. However, the initial conditions were not always as symmetric as in the case of simulations. For example,
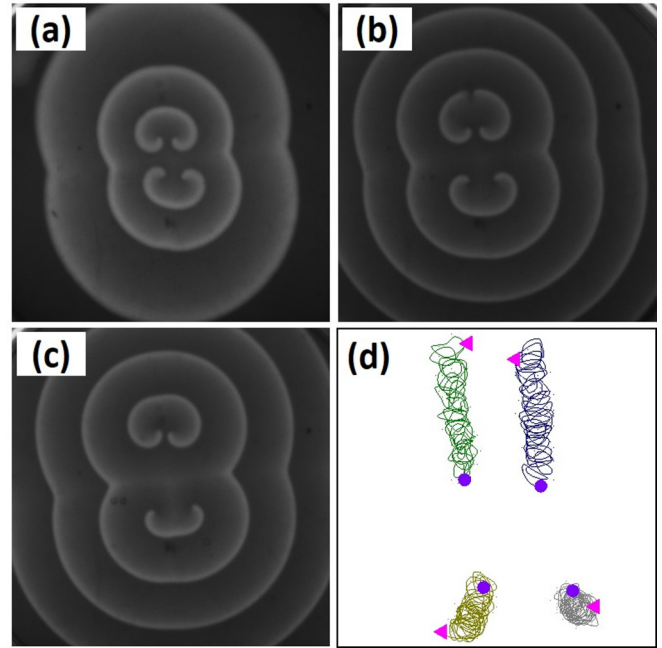

FIG. 7. Repulsion between two pairs of spiral waves. Snapshots at (a) 19 min, (b) 88 min, and (c) 174 min after initiation of the reaction. The area of each snapshot is 3.8 cm × 3.8 cm. (d) Tip trajectories showing repulsion. The circles and triangles designate the initial and later (at 72.0 min) positions of the individual rotors, respectively. Area shown in box is 0.75 cm × 0.75 cm. Initially $d = 0.295$ cm, $l = 0.31$ cm. A movie of this experiment is available in the Supplemental Material [40] (Mov7).

the distance $l (= 0.185$ cm) in the experiment shown in Fig. 6 is an average of 0.17 cm (top pair) and 0.20 cm (bottom pair). There are several factors for this. The exact instant of multiple target wave initiation by several silver wires may not be perfectly coordinated, due to local microscopic inhomogeneities in hydrogel density or temperature. Once the waves are formed and start to expand, they are cleaved using a thin object. This also involves errors and noise, and however much care is taken, the two l and d values may not be exactly equal as in a simulation.

Figures 6(b)–6(d) depict the time evolution of two spiral pairs leading to annihilation. This is similar to the example shown in Fig. 2. The tip trajectories in Fig. 6(e) portray how a pair of rotors annihilate along the distance l. Here the initial distances are $d = 0.14$ cm and $l = 0.185$ cm. It is to be noted here that attraction leading to annihilation occurs even when the initial distance between the rotors is more than two times the core diameter ($l = 2.05 \times$ core diameter). The same has been observed in the case of numerical studies too. Even though the initial distance in the vertical direction d is smaller than the initial horizontal distance l, the spiral tips attract along the horizontal, once again establishing the fact that the force of attraction is much stronger along the direction of wave motion. In this experiment, however, both l and d are less than $\frac{1}{2}d_c$.

On the other hand, the experiment illustrated in Fig. 7 shows an increasing distance between spiral tips with time. This experiment is an example of spiral repulsion, as earlier
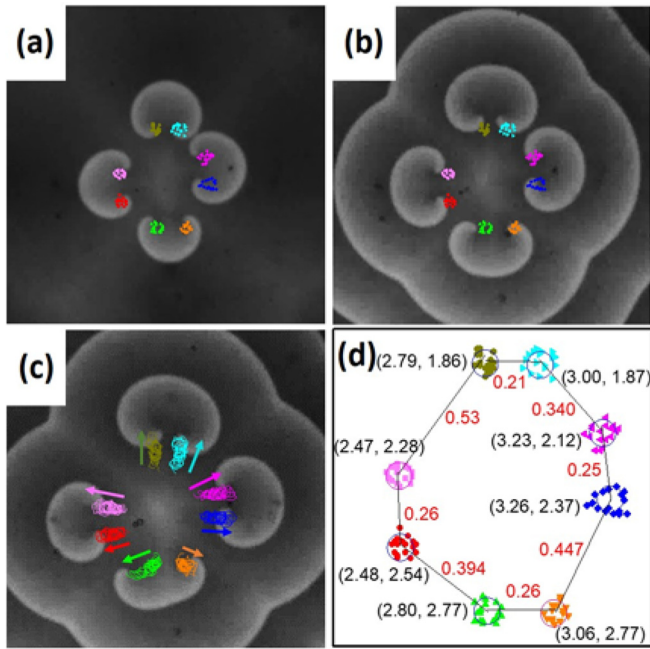
FIG. 8. Repulsion between four pairs of spiral waves. Snapshots covering an area of 2.95 cm × 2.95 cm, at (a) 6.07 min, (b) 56.57 min, and (c) 138.93 min, after the initiation of the reaction. (d) Initial positions of the spiral cores (round curves tracing the dots, which are the positions of the spiral tip during the first rotation of the vortex). The coordinates of the center of the circular cores have been noted in cm (in black), while the distance (in cm) between the center of the cores is given in red. The cores have also been juxtaposed over the snapshots. A movie of this experiment is available in the Supplemental Material [40] (Mov8).
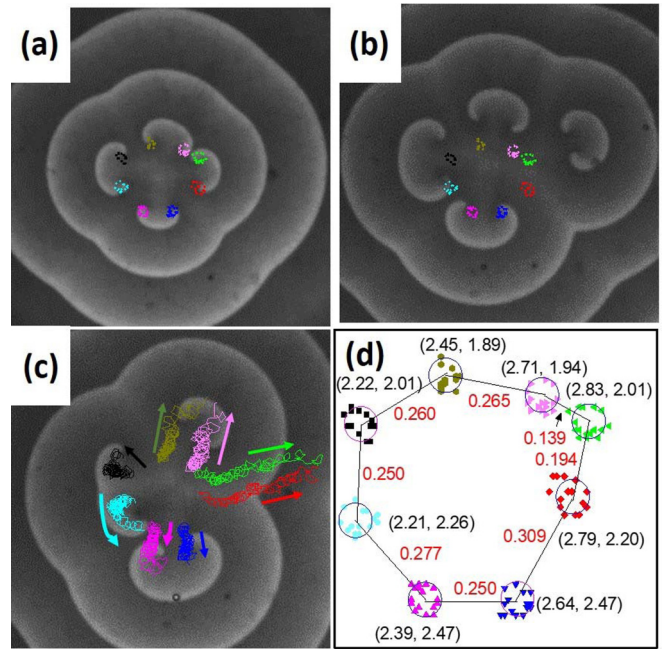

FIG. 9. Annihilation of one pair of rotors following a strong repulsive interaction between four pairs of spiral waves. Snapshots at (a) 19 min (b) 116.1 min, and (c) 188.47 min after initiation of the reaction. Each snapshot covers an area of 2.95 cm × 2.95 cm. (d) Initial positions of the spiral cores with the coordinates of the centers mentioned in cm. The distance (in cm) between the center of each core with its two nearest neighbors is given in red. The initial cores of the eight rotors have also been superimposed over the snapshots. A movie of this experiment is available in the Supplemental Material [40] (Mov9).

seen in our simulations [Fig. 3(c)]. The values of d and l are 0.34 cm and 0.25 cm, respectively. Although the d values are greater than the l values, the tips repel each other vertically. Due to a slight asymmetry in the initial conditions ($l = 0.23$ cm between the top pair, and 0.27 cm between the bottom pair and $d = 0.32$ cm in the left pair and 0.36 cm in the right pair), the symmetry is further broken in the system, as the reaction progresses. The tip trajectories [Fig. 7(d)] exhibit the divergent, yet unsymmetrical, dynamics of the rotors over time. All initial distances here (d and l) lie between $\frac{1}{2}d_c$ and d_c. Hence, the repulsion of the tips are in keeping with our theoretical predictions. Interestingly, one may observe the simultaneous movement of the top spiral pair away from the initial positions, just like a bound state [29].

We also carried out experiments with four spiral pairs. We initiated the waves by cleaving four circular waves generated adjacent to each other, in a square arrangement. The first example is Fig. 8 where only repulsive interaction was observed between the spirals. The d values here ranged between 0.34 cm and 0.53 cm, while the l values ranged in the order of 0.21 cm to 0.26 cm. All d values, except one (0.34 cm on the top right) are greater than the critical distance ($d_c = 0.39$ cm), while the l values are all less than d_c, but greater than $\frac{1}{2}d_c$. One would predict the spiral rotors to repel their twins and not interact strongly with the other neighbors. However, we observe that all the spiral rotors move away from the center,

while (almost) maintaining the initial symmetry. As l values increase very slightly between the tips, the d values are seen to increase more. The only spiral pair that somewhat breaks this symmetry is the one initiated at $y = 2.77$ [shown in Fig. 8(d)], the right tip [initially at (3.06, 2.77)] of which is probably pinned to a small bubble that has been formed at its vicinity seen just below the orange core of the tip in Fig. 8(b)]. This stops its expected movement in the outward direction like the other rotors, while the left tip travels downward, and the l value for this pair increases appreciably.

Figure 9 shows an experiment where a strong repulsive interaction was observed, followed by annihilation of a wave pair. The range of d values in this example is 0.139–0.309 cm, while l ranges between 0.194 cm and 0.265 cm. This system has an inherent asymmetry right from the initiation [Figs. 9(a) and 9(d)]. Hence one might expect some very unique dynamics arising out of the wave interactions. A quick glance at the initial interrotor distances point at only two values ($d = 0.139$ cm in the top-right corner and $l = 0.194$ cm for the right spiral pair) to be in the attractive range. All other distances are in the repulsive zone. The core initiated at (2.83, 2.01) and depicted with green, left-pointing triangles is in the attractive zone of both the cores in its vicinity. So there will be a competition for attracting this one rotor by its two neighbors. As time progresses, the spiral wave pair on the right is expelled farther to the right, by the rest of the rotors [Fig. 9(b)]. This is an

unexpected movement of the green rotor. Even though it was very close to its pink neighbor (core depicted by right-pointing triangles) [Figs. 9(a) and 9(d)], it moved away from it and traveled with its twin (the core of red diamonds). At this stage, the three spiral wave pairs that remain at the center of the reaction chamber display a threefold symmetry among themselves [Fig. 9(b)]. Subsequently, the spiral wave at the top eventually rotates (as a pair) in the clockwise direction, as it also moves away from the center. Meanwhile, the spiral pair which had been expunged to the right moves farther away, and its two rotors start experiencing mutual attraction, and the vortices eventually undergo annihilation at around 138.5 min (after the initiation of the reaction). This annihilation of the wave may be attributed to its l value of 0.194 cm, which is marginally lower than $\frac{1}{2}d_c$. Refer to the movie of the experiment (Mov9) in the Supplemental Material to witness the very interesting wave dynamics of this experiment [40].

VI. DISCUSSION

We have carried out detailed analysis of the interaction of counterrotating spiral pairs. Through our experiments and numerical simulations, we have confirmed what is known about the dynamics of two spiral rotors, and further probed whether it is possible to explain the behavior of more than two spiral vortices, based on spiral wave-pair interactions. We have been able to uncover some previously unexplored behavior which establishes that a simple reduction to spiral pairs fails. Spiral waves, in proximity, would attract each other and finally annihilate. A slight change in initial distance could make two attracting rotors highly repulsive. We have successfully established a critical distance of interaction between the rotor pairs, whether they have a single or multiple neighbors. While the transition from attractive to repulsive interaction occurs across a range of d and l values for more than two rotors, for the simplest case of two rotors, this occurs at 8.2 space units in numerical simulations and 0.195 cm in experiments. As we increase the initial distance further, beyond a particular distance, all interactions between the spirals cease to exist. In numerical simulations the value is 16.4 space units, and for our experiments it was found to be 0.39 cm. This critical distance is equal to the difference of the wavelength of the spiral wave and its core diameter.

Preliminary investigation into the dynamics of interacting spiral rotors for different parameter values, varying initial placement of waveforms, and also different model systems, like the two-variable Oregonator model, have been carried out. The main results reported in our study hold well in all these situations. Across the systems we have observed a priority of attractive interaction between the spiral rotors along the direction of wave motion. For a similar initial condition as ours, it has been seen in numerical as well as experimental experiments that a vortex is being attracted heavily by its twin, sometimes even when the distance separating it from a neighboring rotor (belonging to another spiral wave pair) was much lower (Fig. S7 [40]).

We also observed some very interesting symmetry-breaking dynamics of the spiral waves. Existing literature supports the phenomenon of symmetry breaking in two- and three-component reaction diffusion processes. The dominance

of one spiral over the other in a spiral pair, leading to symmetry breaking, was earlier demonstrated in numerical simulations [25,26], as well as in experiments [27]. With our experiments and simulations, we show that a system with multiple spirals, all having the same frequency initially, can also undergo symmetry-breaking dynamics, even if the initial distances separating them are equal, leading to an uneven geometry as time progresses. We show that in our system, the spiral tips keep on rotating with the same frequency (or time period), while they trace unsymmetrical trajectories, leading to an overall asymmetry in the system, without any necessary dominance of one tip over the other. Unlike the results shown in [27], the cores of our spirals remain fixed at the no-interaction zone, and there is no visible oscillation of the intercore distance. While some groups [23,29] claim that a three-component model is required to show the symmetry-breaking instability of spiral pairs, Ruiz-Villarreal *et al.* [27] have shown that such an instability is indeed possible in a two-component FitzHugh-Nagumo model. The former groups believe that the symmetry breaking requires the presence of a third field whose feedback results in strong interaction between the spiral rotors [23]. However, the results presented in our current study seem to support those by Ruiz-Villarreal *et al.* [27], as we successfully demonstrate the symmetry breaking instability in a two-variable Barkley model system. The parameter range through which the two-variable Barkley model displays the symmetry breaking is also substantial. Spontaneous symmetry breaking can still be observed for a set of parameters entirely different from our current set ($a = 1.1, b = 0.18, \epsilon = 0.01, dt = 0.012, dx = 0.35, D_u = 1.0, D_v = 0.0$ as shown in Fig. S7 [40]). This set of parameters with nondiffusing recovery variable ($D_v = 0.0$) is often chosen to model systems, where the catalyst is immobilized [29,36]. All the observations made with our parameter values can also be observed in this system. However, it may be expected that the exact value of the critical distance may change with changing parameters. A simple change in the value of the excitability parameter ϵ changes the nature of the spirals (time period, frequency, wavelength, and tip trajectory or core size) [17]. Hence, it can be expected that the critical distance might also change under these circumstances, though it will always be less than one wavelength. For both the sets of parameter values that we have thoroughly investigated, we observed the formation of bound states by some pairs of counterrotating spirals (Figs. 3, 5, and S7). This is in keeping with results shown in [29]. Similar observations have also been made in many of our experiments (Figs. 7–9). However, a sudden asymmetry in the system brought about by some local inhomogeneities may result in the bound states losing their stability. The spiral pairs in these cases may attract and annihilate Figs. 3(b), 5, and 9, or even repel (Fig. S3), after having travelled as a bound state for a long distance. Reducing the grid size does hasten the onset of the symmetry-breaking instability (as mentioned in [27]), and increasing grid sizes lead to a more symmetric system. However, for multiple spirals (more than two), we found that symmetry breaking is observed even for high grid sizes (0.5 space units). Our experiments show that symmetry breaking is an inherent quality of excitable systems with multiple excitable centers. The results of our numerical simulations are

in keeping with that idea. The presence of numerical noise in simulations or microscopic variation of system parameters in experiments can make a system starting from symmetrical initial conditions evolve into one of striking asymmetry, as time progresses. An initial dissymmetry, however small, blows up with time, and the system diverges into complete asymmetry.

Some initiatory simulations by varying the phase of the two spiral rotors were also carried out. In all our simulations described so far, the counterrotating spirals had the same initial phase [consider their amplitude along the y direction for a pair of spirals placed side by side, like in Fig. 1(c), as depicted clearly in Fig. 5 of [42]]. For counterrotating spirals with an initial phase difference of π, the nature of interaction between the spiral tips depends upon the mutual orientation of the waveforms and the distance separating the tips. When there is an additional wave between the two tips (apart from their immediate spiral arms), they will not attract, however close they may be initiated. This happens even when the phase difference between the two rotors is zero or 2π [30,40]. However, if we can initiate the two tips in such a way that they do not have any intervening wave, the tips may attract and annihilate. Refer to our Supplemental Material (Fig. S8) for results of some preliminary simulations. It will be interesting to further explore if there is an oscillatory dependence of the nature of interaction on the phase difference of two spiral rotors.

The results obtained for the interactive behavior of these two-dimensional spiral waves are somewhat different from that known about their three-dimensional counterparts, the scroll waves. These three-dimensional scroll waves can be thought to be a stack of spirals, or an extension of a two-dimensional spiral along the third dimension. When neighboring scrolls approach each other, their constituent spirals can annihilate if they have opposite sense of rotation. Depending on the distance between the filaments, such a phenomenon can lead to "reconnection" of the scroll waves. In experiments with scroll rings, we had in an earlier study [33] shown that the circular filaments attract each other and reconnect, when they are less than one core diameter apart. Repulsion between the wave forms was also found for a particular orientation of the filaments, which was believed to be due to the proximity of corotating spirals. Scroll rings having positive filament tension undergo spontaneous shrinkage and eventually disappear. Hence, it is difficult to establish quantitatively the repulsive influence of the constituent spirals on the dynamics of two neighboring scroll rings. In another experimental study of parallel and straight scroll waves [35], it was shown that they repel each other when they are separated by distances greater than $\frac{2}{3}\lambda$ but smaller than one wavelength. Here the authors could not initiate pairs of scroll waves that were closer than $\frac{2}{3}\lambda$ in their experiments. Hence, for three-dimensional scroll waves, a critical distance for the sudden flipping of attractive interaction to give way to repulsion is not yet known in the literature. However, in our current study we observe that the attraction between rotors is felt over a distance that is many times more than the core diameter. Numerically, for our chosen parameters, the distance was found to be 4.5 times the core diameter, while experimentally we have observed attractive interaction at least up to 2.2 times the core diameter (both of which are close to half a wavelength).

It would be interesting to probe the system of 3D scroll waves to ascertain if its constituent spirals also attract until such distances that are close to half of a wavelength.

VII. CONCLUSIONS

In conclusion, we have successfully quantified the nature of spiral wave interaction as a function of wave properties. A critical distance of interaction of two spiral waves has been established. This measure could be used to understand the dynamics of multiple rotors. For systems of two, four, and eight spiral cores, we have demonstrated the possibilities of spiral attraction leading to annihilation, repulsion, and no interaction. As the number of rotors are increased, more complicated dynamics come to light. In the presence of additional rotors, a pair of spirals in the repulsive zone can undergo attraction followed by annihilation. Spontaneous symmetry breaking is also observed, inducing the spiral tips to trace intriguing tip trajectories. We have validated by several examples and comparisons that the dynamics of the spiral rotors also depend on the motion of the spiral wave arm. If the initial waves are moving away from each other, the rotors that will originate from the two ends of a single wave attract each other more strongly than they do other rotors from neighboring spiral waves.

Spiral rotors of these kind play a vital role in the fibrillatory conduction of the cardiac muscles, by activating the atria at exceedingly high frequencies [10]. The present study illuminates the nuances of spiral wave interaction and may facilitate a better understanding of the interaction of rotors in the atria and ventricles. Since we have shown how the interaction of neighboring spiral tips can bring about their drift within the excitable media, or their annihilation, our results have strong implications in understanding the dynamics of such rotors in the cardiac system. The drift of otherwise non-meandering spiral rotors due to interaction with nearby spirals can transform a monomorphic tachycardia into polymorphic tachycardia, and even the life-threatening Torsades de pointes, in the presence of several rotors. Contrarily, mutual attraction of rotors leading to annihilation of spiral pairs, will point towards the quenching of tachycardia or fibrillation in the heart muscles.

Further analysis of the velocity of attraction and repulsion should shed more light on the interaction dynamics. It remains to be seen whether the velocity of these interactions would take the form of Yukawa potentials, as was found in the case of three-dimensional scroll rings [33,43]. Future studies could try to uncover the cause of the symmetry-breaking dynamics that is observed in systems with multiple spiral rotors. Another interesting question is how the spiral velocity fields change as a function of model parameters. Also, detailed simulations on interaction of spirals with varying phase difference, for both counter- and corotating spirals, will be worth exploring.

[1] J. Jalife, M. Delmar, J. Anumonwo, O. Berenfeld, and J. Kalifa, *Basic Cardiac Electrophysiology for the Clinician*, 2nd ed. (Wiley-Blackwell, Oxford, 2009).

[2] F. H. Fenton, E. M. Cherry, and H. M. Hastings, Chaos **12**, 852 (2002).

[3] F. X. Witkowski, L. J. Leon, P. A. Penkoske, W. R. Giles, M. L. Spano, W. L. Ditto, and A. T. Winfree, Nature (London) **392**, 78 (1998).

[4] J. Christoph, M. Chebbok, C. Richter, J. Schröder-Schetelig, P. Bittihn, S. Stein, I. Uzelac, F. H. Fenton, G. Hasenfuß, R. F. Gilmour Jr., and S. Luther, Nature (London) **555**, 667 (2018).

[5] S. Luther, F. H. Fenton, B. G. Kornreich, A. Squires, P. Bittihn, D. Hornung, M. Zabel, J. Flanders, A. Gladuli, L. Campoy, E. M. Cherry, G. Luther, G. Hasenfuss, V. I. Krinsky, A. Pumir, R. F. Gilmour, Jr., and E. Bodenschatz, Nature (London) **475**, 235 (2011).

[6] O. Steinbock, F. Siegert, S. C. Müller, and C. J. Weijer, Proc. Natl. Acad. Sci. USA **90**, 7332 (1993).

[7] I. R. Epstein and J. A. Pojman, *An Introduction to Nonlinear Chemical Dynamics: Oscillations, Waves, Patterns, and Chaos* (Oxford University Press, Oxford, 1998).

[8] S. Jakubith, H. H. Rotermund, W. Engel, A. von Oertzen, and G. Ertl, Phys. Rev. Lett. **65**, 3013 (1990).

[9] J. Lechleiter, S. Girard, E. Peralta, and D. Clapham, Science **252**, 123 (1991).

[10] J. Jalife, R. A. Gray, G. E. Morley, and J. M. Davidenko, Chaos **8**, 79 (1998).

[11] O. Steinbock and S. C. Müller, Int. J. Bifurcation Chaos Appl. Sci. Eng. **3**, 437 (1993).

[12] K. I. Agladze, Chaos **6**, 328 (1996).

[13] J. Schütze, O. Steinbock, and S. C. Müller, Nature (London) **356**, 45 (1992).

[14] J. Schlesner, V. S. Zykov, H. Brandtstädter, I. Gerdes, and H. Engel, New J. Phys. **10**, 015003 (2008).

[15] M. Braune and H. Engel, Phys. Rev. E **62**, 5986 (2000).

[16] J. Jalife, J. Cardiovasc. Electrophysiol. **14**, 776 (2003).

[17] D. Mahanta, N. P. Das, and S. Dutta, Phys. Rev. E **97**, 022206 (2018).

[18] S. Dutta and O. Steinbock, Phys. Rev. E **83**, 056213 (2011).

[19] B. T. Ginn and O. Steinbock, Phys. Rev. Lett. **93**, 158301 (2004)

[20] S. Dutta and O. Steinbock, J. Phys. Chem. Lett. **2**, 945 (2011).

[21] F. M. Zanotto and O. Steinbock, Phys. Rev. E **103**, 022213 (2021).

[22] E. Nakouzi, J. F. Totz, Z. Zhang, O. Steinbock, and H. Engel, Phys. Rev. E **93**, 022203 (2016).

[23] I. Aranson, H. Levine, and L. Tsimring, Phys. Rev. Lett. **76**, 1170 (1996).

[24] N. Tomii, M. Yamazaki, T. Arafune, K. Kamiya, K. Nakazawa, H. Honjo, N. Shibata, and I. Sakuma, Am. J. Physiol.: Heart Circ. Physiol. **315**, H318 (2018).

[25] E. A. Ermakova, A. M. Pertsov, and E. E. Shnol, Physica D **40**, 185 (1989).

[26] I. Aranson, L. Kramer, and A. Weber, Physica D **53**, 376 (1991).

[27] M. Ruiz-Villarreal, M. Gómez-Gesteira, C. Souto, A. P. Muñzuri, and V. Pérez-Villar, Phys. Rev. E **54**, 2999 (1996).

[28] R. R. Aliev, V. A. Davydov, T. Kusumi, and T. Yamaguchi, Netsu Sokutei **24**, 194 (1997).

[29] I. Schebesch and H. Engel, Phys. Rev. E **60**, 6429 (1999).

[30] J. F. Totz, H. Engel, and O. Steinbock, New J. Phys. **17**, 093043 (2015).

[31] R. M. Zaritski and A. M. Pertsov, Phys. Rev. E **66**, 066120 (2002).

[32] B. Vasiev, F. Siegert, and C. Weijer, Phys. Rev. Lett. **78**, 2489 (1997).

[33] N. P. Das and S. Dutta, Phys. Rev. E **91**, 030901(R) (2015).

[34] D. Mahanta and S. Dutta, Phys. Rev. E **100**, 022222 (2019).

[35] J. Kupitz and M. J. B. Hauser, J. Phys. Chem. A **117**, 12711 (2013).

[36] D. Barkley, Physica D **49**, 61 (1991).

[37] H. Dierckx, I. V. Biktasheva, H. Verschelde, A. V. Panfilov, and V. N. Biktashev, Phys. Rev. Lett. **119**, 258101 (2017).

[38] N. P. Das and S. Dutta, Phys. Rev. E **96**, 022206 (2017).

[39] S. Alonso, Ralf Kahler, A. S. Mikhailov, and F. Sagués, Phys. Rev. E **70**, 056201 (2004).

[40] See Supplemental Material at http://link.aps.org/supplemental/10.1103/PhysRevE.105.054213 for movies of experiments (corresponding to Figs. 6, 7, 8, and 9) and some additional numerical data.

[41] O. Steinbock, C. T. Hamik, and B. Steinbock, J. Phys. Chem. A **104**, 6411 (2000).

[42] G. Byrne, C. D. Marcotte, and R. O. Grigoriev, Chaos **25**, 033108 (2015).

[43] M.-A. Bray and J. P. Wikswo, Phys. Rev. Lett. **90**, 238303 (2003).